

## Analysis of the Thermal Equilibrium State of Bunched Beams with a Streak Camera

I. Hofmann, K. F. Johnson,\* P. Spiller, H. Eickhoff, G. Kalisch, W. Laux, and M. Steck  
*Gesellschaft für Schwerionenforschung Darmstadt m.b.H., P.O. Box 110552, D-64220 Darmstadt, Germany*  
 (Received 25 August 1995)

The thermal equilibrium distribution of cooled bunched ion beams in the ESR storage ring is investigated in simultaneous longitudinal-transverse measurements by using a scintillator and streak camera in the extraction beam line. We have found a cylindrical bunch model with local Gaussian density profiles confirming the model of a Maxwell-Boltzmann distribution in six-dimensional phase space.

PACS numbers: 29.20.-c, 29.27.Bd, 41.85.Ew

In many applications of intense charged particle beams, such as heavy ion fusion, spallation neutron sources, radioactive waste transmutation, and others, knowledge of the space charge distribution in all three dimensions is required in order to determine the ultimate intensity performance and possible sources of phase space dilution. Furthermore, recent bunched beam experiments with electron cooling near the space charge limit [1,2], and evidence of bunched beam laser cooling in storage rings [3], have suggested that for a complete interpretation of the data and possibly an application of these techniques to crystalline beams [4] it would seem highly desirable to measure the three-dimensional bunch shape.

In view of this fundamental interest in time and space resolved measurements we have applied the streak camera technique frequently used in plasma physics and in electron storage rings (ESR's) [5] to the environment of an ion storage ring. Contrary to ESR's, where synchrotron radiation allows a nondestructive diagnostic, we have to employ scintillators in the extraction line. This has enabled us, in particular, to perform correlated measurements between time and horizontal deviations. Prior to extraction from the ESR the bunches have been cooled by electron cooling to a stationary state on a time scale of seconds. In principle the equilibrium state is the result of a competition between electron cooling and heating by intrabeam scattering and possibly machine resonances due to a finite space charge tune shift.

Theoretical investigations frequently assume a "thermal" distribution where particles are in a thermodynamic equilibrium described by a Maxwell-Boltzmann distribution [6,7]. In principle a sufficient amount of "collisionality" is needed in order to reach such a state of thermodynamic equilibrium and it is not *a priori* clear whether the competing mechanisms in an ion storage ring would not prevent this. It should be noted here that injection of a bunch into a linac or storage ring can produce an initial distribution, which is far from a thermodynamic state and where even in one degree of freedom the notion of temperature is inappropriate. This is the case, for instance, if the transverse velocity spread is not a constant along the bunch due to injection conditions or losses

on the aperture. The latter have been encountered occasionally in our measurements if the beam was not guided properly through the extraction channel. The scope of our streak camera experiments has been in particular to verify experimentally the Maxwell-Boltzmann distribution for an electron cooled bunched beam and demonstrate the potential of this technique for further future applications.

The ESR extracted bunches were studied by measuring the light produced on a scintillator inserted into the beam path at an angle of  $45^\circ$  with respect to the beam axis. The scintillator was placed in the extraction beam line for reinjection into the SIS synchrotron, some 40 m away from the ESR. The material chosen was a 0.5 mm thick sheet of NE102A, which is a widely used plastic scintillator with good light output and high temporal resolution due to its decay constant of 2.4 ns. Its main disadvantage is saturation, which can be overcome by expanding the beam spot. The streak camera used was a Hamamatsu C2830. The scintillator spot was viewed by a 100  $\mu\text{m}$  wide slit oriented horizontally and centered in vertical direction. The slit is imaged on a photocathode converting the light image into an electron image. The latter is deflected vertically by a time varying field and

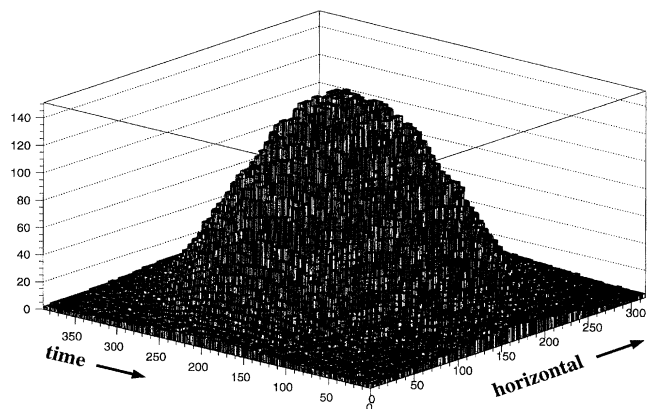


FIG. 1. Histogram of streak camera image of electron cooled  $\text{C}^{6+}$  bunch at 250 MeV/u. Time units in pixels (2.23 ns/pixel); horizontal units in pixels (not calibrated).

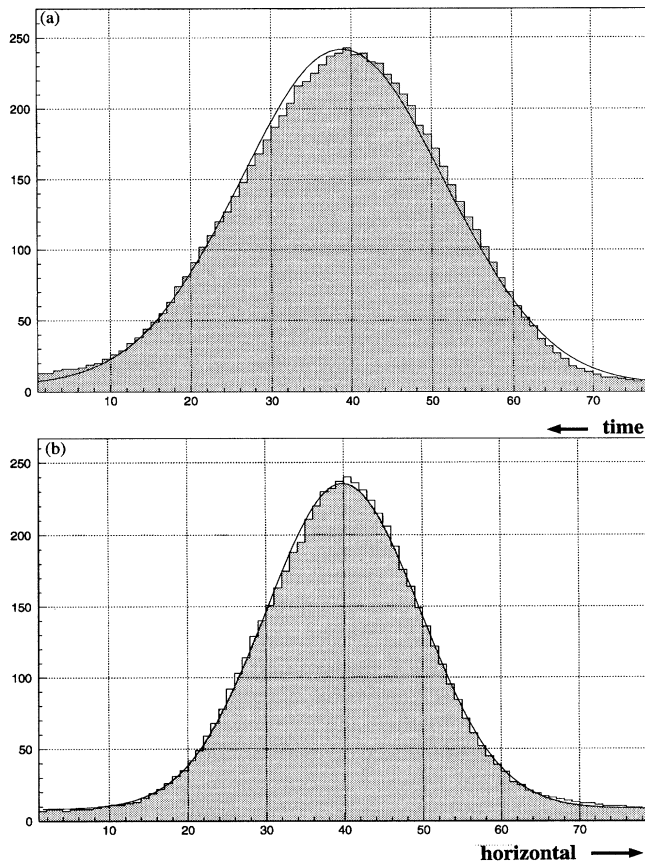


FIG. 2. Longitudinal cut (top) and horizontal cut (bottom) through bunch center for  $C^{6+}$  bunch with Gaussian fits. Units in pixels (2.23 ns/pixel; horizontal uncalibrated).

reconverted into a light image within a charge-coupled-device (CCD) camera. Hence the sweep from top to bottom represents the time axis flow of a horizontal cut through the beam center.

The histogram of a streaked image of a  $C^{6+}$  cooled bunch with 1.15 mA (distributed over two bunches) is shown in Fig. 1. The CCD screen has a resolution of  $512 \times 512$  pixels. Cuts through the bunch center indicate Gaussian profiles both in horizontal and longitudinal direction as shown in Fig. 2. It is noted that the horizontal cut agrees very well with a Gaussian fit taking into account the offset due to a constant background. The streak camera resolution is 2–3 pixels horizontally. The longitudinal cut shows a slightly increasing background offset with increasing time (i.e., to the left, noting that in our representation time pixels are in reversed time direction). This indicates that there is a small, but negligible afterglow effect of the scintillator. Cuts at different times or horizontal positions also show Gaussian profiles. An absolute time calibration is possible by recording the light from two bunches, which have an

accurately defined time distance given by the rf frequency (3.403 MHz), hence we obtain 2.23 ns/pixel. The  $2\sigma$  time width of the bunch in Fig. 2 is equivalent to 55 ns. We note that the time profile is inevitably stretched by the intrinsic time resolution of the streak camera, which is given by the width of the  $100 \mu\text{m}$  slit on the CCD screen (estimated to 10 pixels) times the ratio of the effective streak time to the effective number of pixels (here 480). For the actually used streak time of 1000 ns we thus obtain a time resolution of 17 ns, hence the real time width of the bunch must be assumed to be reduced by this amount. In principle the time resolution could be made as short as the scintillator light decay constant (2 ns) by choosing a correspondingly shorter streak time. Since the streak camera is triggered to the kicker loading event and the actual kick can jump by the bunch distance time (here 294 ns) the camera would then have frequently missed the bunch for such high resolution measurements. The horizontal resolution, on the other hand, is estimated to 2–3 pixels, which is sufficiently accurate for evaluating our measurements. An absolute calibration of horizontal size is less straightforward. By a comparison with the scintillator edge we have determined the actual horizontal width of the above example as 3 mm. If the beta function is sufficiently well known at the place of the scintillator, the emittance can be directly calculated in absolute units from the width of the beam, which will be the subject of future measurements.

In another series of measurements in different beam times with  $Ne^{10+}$  as well as  $C^{6+}$  beams of the same kinetic energy (250 MeV/u) and currents of typically 1 mA we have obtained, however, significant deviations from Gaussian profiles (see Fig. 3). Such profiles might be explained as a result of scintillator saturation if the deposited energy would have been significantly larger than in the  $C^{6+}$  measurements shown in Fig. 2, which was

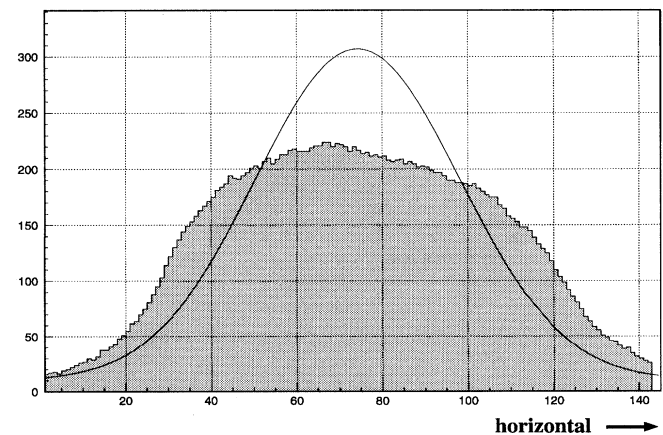


FIG. 3. Non-Gaussian horizontal profile at bunch center for  $Ne^{10+}$  bunch explained by large horizontal width and beam striking the aperture or extraction septum.

not the case. A more likely explanation is that a much larger horizontal width caused possibly by a different extraction optic or a reduced electron cooling effect has caused beam edge losses at an aperture limitation beyond extraction, and the edge has rotated to the beam center (horizontally) further downstream in the extraction channel, where the scintillator was placed. We have thus discarded such cases for further evaluation.

We have evaluated quantitatively the horizontal width by Gaussian fits and plotted the  $1\sigma$  deviation against time (in pixels), i.e., longitudinal position. This is compared in Fig. 4 with the intensity curve obtained by summing up at each time pixel the intensities of all horizontal channels. Note that the bunch of Fig. 1 corresponds to the right hand profile of Fig. 4. It is noted that the error of the width in the Gaussian fit is increasing for smaller intensities at the bunch boundaries, where the background is dominating. In this example and in all other cases evaluated we have found that the beam width is constant within  $\pm 5\%$  over  $\pm 2\sigma$  of the intensity profile. This observation—along with the Gaussian profiles in all cuts—allows us to conclude that we deal with a “cylindrical bunch model” as opposed to “ellipsoidal” or other bunch models.

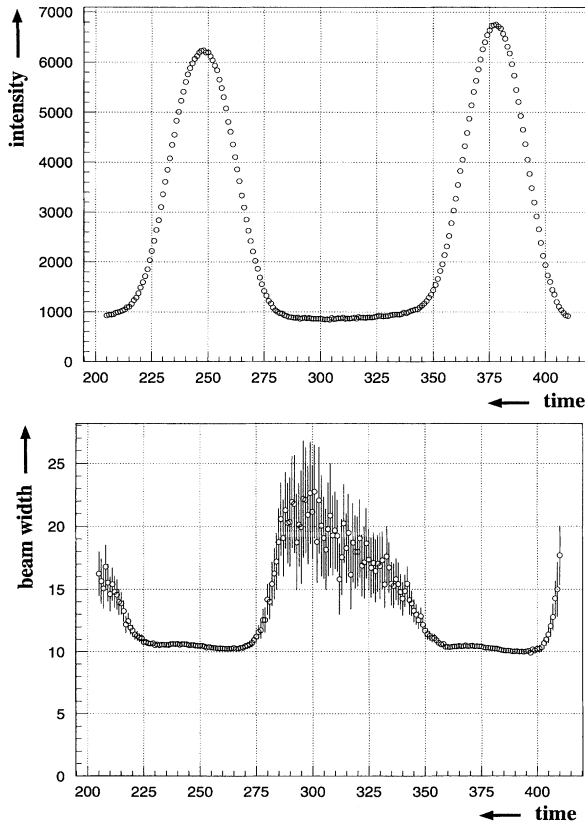


FIG. 4. Intensity (horizontally integrated) vs time (top) and bunch width vs time (bottom) for  $C^{6+}$  double bunch. Units in pixels (2.23 ns/pixel; beam width uncalibrated).

In the following we summarize the properties obtainable from a Maxwell-Boltzmann distribution relevant to our measurements, where we follow the notation of Ref. [7]:

$$f = c_0 \exp(-H_{\perp}/k_B T_{\perp}) \exp(-H_{\parallel}/k_B T_{\parallel}). \quad (1)$$

We have assumed here constant focusing (“smooth approximation”) and allowed for different temperatures in the transverse and longitudinal degrees of freedom. This agrees with the observations in storage rings, where intra-beam scattering leads to different temperatures depending on the details of the focusing and dispersion functions. In the laboratory frame the Hamiltonians are defined as

$$\begin{aligned} H_{\perp} &= \gamma_0 \frac{m}{2} v_{\perp}^2 + q\Phi_{\perp}, \\ H_{\parallel} &= \gamma_0^3 \frac{m}{2} (\Delta v_{\parallel})^2 + q\Phi_{\parallel}, \end{aligned} \quad (2)$$

with  $\Delta v_{\parallel} \equiv v_{\parallel} - v_0$ . In general the potentials are a sum of the external potentials (focusing and rf potential well) and the self-consistently calculated space charge potentials.

A fundamental property of the Maxwell-Boltzmann distribution is the spatial independence of velocity spreads independent of the particular shape of the potentials, which follows from the factorization of the kinetic and potential parts in the Maxwell-Boltzmann distribution. As usual we multiply  $f$  by  $v^2$  and obtain by integration over velocity space and appropriate normalization the familiar result

$$\overline{v_{\perp}^2} = 2k_B T_{\perp} / \gamma_0 m, \quad \overline{v_{\parallel}^2} = k_B T_{\parallel} / \gamma_0^3 m, \quad (3)$$

which is independent of  $z$  (and of  $x, y$ ). Equations (3) thus yield the definition of temperatures in an equilibrium sense as global properties. Note that according to Ref. [7] the beam frame temperatures are given by  $\gamma_0 T$ .

For our measurements we have estimated the effect of space charge on these potentials as less than 5% longitudinally and less than 1% transversely. Space charge can thus be ignored, and we therefore deal with emittance dominated beams. For this special case the radial density profile is readily obtained as

$$n(r)/n(0) = \exp(-\omega_0^2 Q_0^2 r^2 / 2k_B T_{\perp}) \quad (4)$$

and the line density as

$$\rho(z)/\rho(0) = \exp(-q\Phi_{\parallel 0} z^2 / k_B T_{\parallel} z_0^2), \quad (5)$$

where we have assumed a harmonic rf potential  $\Phi_{\parallel} = \Phi_{\parallel 0}(z^2/z_0^2 - 1)$  and a transverse potential given by the betatron tune  $Q_0$ :  $\Phi_{\perp} = \omega_0^2 Q_0^2 r^2 / 2q$ , with  $\omega_0$  the revolution frequency. A crucial point is the independence of the transverse density profile on  $\overline{z^2}$ , which is a direct consequence of the constancy of  $\overline{v_{\perp}^2}$  in the absence of transverse space charge effects.

Hence we find that our measurements strongly support the assumption of a Maxwell-Boltzmann distribution and a cylindrical shape for the cooled bunches. Because of a

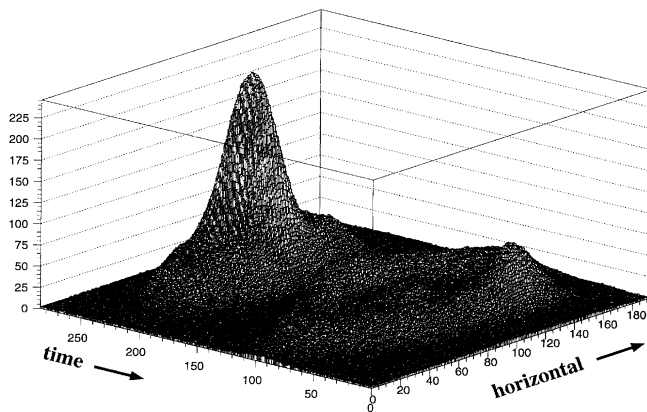


FIG. 5. Unstable  $C^{6+}$  bunches for increased ion intensities subject to electron cooling.

lack of precise emittance measurement in absolute units we have been able to estimate only that longitudinal and transverse agree within a factor of about 2. The cylindrical shape has an important influence on the geometry factor for calculating the longitudinal self-consistent electric field on axis. For a beam of radius  $R_b$  in a pipe of radius  $R_p$  it is given by (see, for instance, Ref. [8]):  $g = 1 + 2\ln R_p/R_b$  and thus independent of the position along the bunch. A further consequence of the constant emittance along the bunch is that the space charge incoherent tune shift must be expected to follow the Gaussian intensity profiles.

For completeness we mention that in the case of a space charge dominated bunch obeying a Maxwell-Boltzmann distribution the spatial shape is expected to become more ellipsoidal. In the longitudinal space charge limit the line density approaches the shape of the confining harmonic potential due to the Debye shielding effect [9]. Such a parabolic line density was measured for space charge dominated electron bunches at low energy [10]. Assuming that also the transverse space charge limit is achieved, where the space charge force exactly cancels the applied focusing, we obtain  $n(r) \equiv n(0)$  independent of  $z$ .

We thus readily find an ellipsoidal boundary at the space charge limit given by  $R_b(z)^2 = R_b(0)^2(1 - z^2/z_0^2)$ , if we ignore the logarithmic dependence of the geometry factor on  $R_b$ . Detailed numerical calculations for ellipsoidal bunches and a determination of the proper effective geometry factor have recently been presented in Ref. [11].

Streak camera investigations for such space charge dominated ion bunches in a storage ring might be possible in the near future if laser cooling can be shown to reduce the transverse emittance to the necessary small values, which are far beyond conventional storage ring operation. We mention that we have also applied the streak camera to study bunches subject to instabilities, which have generally been observed in the ESR for currents exceeding 2–3 mA without clear identification of the underlying mechanism. An example demonstrating the capabilities of this technique is shown in Fig. 5. After having gone through an unstable phase of the two bunches the electron cooling has just started to become effective at the bunch centers prior to extraction.

---

\*Permanent address: LANL, Los Alamos, NM 87545.

- [1] T.J. Ellison *et al.*, Phys. Rev. Lett. **70**, 790 (1993).
- [2] S.S. Nagaitsev *et al.*, in *Proceedings of the Workshop on Beam Cooling and Related Topics, Montreux, Switzerland, 1993* (CERN, Geneva, 1994).
- [3] J. Hangst *et al.*, Phys. Rev. Lett. **74**, 4432 (1995).
- [4] A. Rahman and J.P. Schiffer, Phys. Rev. Lett. **57**, 1133 (1986).
- [5] C. Bovet, in *Proceedings of EPAC 92: Third European Particle Accelerator Conference, Berlin, 1992* (Editions Frontiers, Gif-sur-Yvette, France, 1992), p. 259.
- [6] J.D. Lawson, *The Physics of Charged Particle Beams* (Clarendon, Oxford, 1988), 2d ed., Chap. 4.6.
- [7] M. Reiser and N. Brown, Phys. Rev. Lett. **71**, 2911 (1993).
- [8] M. Reiser, *Theory and Design of Charged Particle Beams* (Wiley & Sons, New York, 1994), p. 498ff.
- [9] I. Hofmann and J. Struckmeier, Part. Accel. **21**, 69 (1987).
- [10] D.X. Wang *et al.*, Appl. Phys. Lett. **62**, 3232 (1993).
- [11] C.K. Allen, N. Brown, and M. Reiser, Part. Accel. **45**, 149 (1994).